



A Neurodynamic Algorithm for Energy Scheduling Game in Microgrid Distribution Networks

Shifan Wen^{1,2} · Xing He¹

Accepted: 26 August 2021 / Published online: 2 September 2021
© The Author(s), under exclusive licence to Springer Science+Business Media, LLC, part of Springer Nature 2021

Abstract

In this paper, a competitive energy scheduling strategy game of N -microgrids (MGs) inside a distributed network is considered. Each microgrid (MG) aims to maximize its profit under the noncooperative game frame. The strategy-making of each MG depends on its equipment constraints, the aggregate energy supplies of all MGs, and the energy balance of supplies and demands. To solve above discussed problem, a noncooperative game with linear coupled constraints and a distributed neurodynamic algorithm are proposed to seek the generalized Nash equilibrium (GNE). Besides, the correctness and convergence of the proposed algorithm are analyzed in detail. The effectiveness and feasibility of the proposed method are also illustrated via the simulation example.

Keywords Neurodynamic algorithm · Energy scheduling game · Microgrid distribution network

1 Introduction

Though the advance of industry forces rapid economic development, it also brings many challenges to the environment and resources. To improve the energy scheduling between traditional and renewable energy, the construction of the MG becomes vitally significant [1]. It is crucial to develop a safe, stable and efficient modern power system, in which the stability, flexibility, and the balance of the supply and demand side are guaranteed [2].

Recently, energy management has been investigated widely to allocate energy optimally and construct a safe and stable power grid. A smart energy management system (EMS) coordinates the working of distributed generators and energy storage system (ESS

✉ Xing He
hexingdoc@swu.edu.cn

Shifan Wen
shifanwen92@gmail.com

¹ Chongqing Key Laboratory of Nonlinear Circuits and Intelligent Information Processing, College of Electronic and Information Engineering, Southwest University, Chongqing 400715, China

² School of Economic Information and Engineering, Southwestern University of Finance and Economics, Chengdu 611130, China

and achieves the maximum benefits of the MG system [3,4]. Typically, the control mode of EMS is mainly centralized control. To minimize the emission cost of greenhouse gases, energy costs, and maximize the output of renewable power, a centralized method has been used to coordinate the energy management between the MG and the main power grid [5]. However, the centralized control can not provide a formidable computing ability to deal with a volume of data and suffers from single-point fault and privacy disclosure.

Nowadays, numerous studies have been conducted in the distributed optimization of microgrid energy management. Compare with centralized energy management, the distributed optimization provides a more efficient and reliable energy management strategy for the microgrid system (MGS) [6–9]. In [6], a real-time energy market of the multi-MGs is optimized by a distributed robust algorithm. A distributed algorithm is proposed to solve the economic dispatch problem, in which some groups of generator units are considered [7]. Reference [8] proposes a distributed neuro-dynamic optimization algorithm for energy internet management. In [9], a distributed-consensus based algorithm is proposed to solve the economic dispatch problem in the MG.

Game theory has been broadly applied in society and resource environment models [10], network congestion control (NCC) [11–13], and energy management [12,14–16]. In [14], a cooperative game is applied in Multi-MGs for energy and reserve dispatch. However, individuals practically care about the maximization of their own interests, which can be fully illustrated by the noncooperative game. Reference [12] considers a population of noncooperative agents, the cost functions of all competitors are related to the average population status and the sharing constraints, the proposed method is applied in NCC and demand-side management. An aggregative game is applied to model and analyze the electric consumption control in the smart grid [15] and solve a day-ahead electric vehicle charge problem [16].

Consider the distributed optimization of MG system and game theory approach for energy management in the existing works, the main contributions of this paper are given as follows.

- (1) A noncooperative game is applied to model the practical relationships of the microgrid distribution network. Each MG is independent, however, the energy supplies and profits are closely related to others. Under the coupled constraints, the equilibrium seeking is completed by the proposed neurodynamic algorithm.
- (2) The proposed distributed neurodynamic algorithm can effectively solve the game problem with linear coupled constraints.
- (3) The correctness and convergence of the proposed algorithm are also analyzed by a comprehensive theoretical analysis.

The rest is organized below. Section 2 gives some needed preliminaries and related mathematical notations. In Sect. 3, the mathematical models of the basic energy units are described. Section 4 gives the game model of the discussed problem and the detailed analysis of the proposed distributed neurodynamic algorithm. The simulation example and conclusion are given in Sects. 5 and 6, respectively.

2 Notations and Preliminaries

In this section, some notation definitions and preliminary knowledge are given as follows:

2.1 Notational Conventions

In this paper, R^n and $\|\cdot\|$ denote the n -dimensional real column vector and the Euclidean norm, respectively. $1_n = (1, \dots, 1)^T \in R^n$. $\xi_1 \pm \xi_2 = \{\varpi_1 \pm \varpi_2 \mid \varpi_1 \in \xi_1, \varpi_2 \in \xi_2\}$ present the Minkowski sum or minus of the sets ξ_1 and ξ_2 . $rint(\xi)$ presents the relative interior of the convex set ξ [17].

2.2 Preliminaries

In this section, some basic mathematic descriptions of the graph theory, convex analysis, and variational inequality are given as follows:

Defining the graph $\mathcal{G} = (\mathbb{N}, \mathbb{E})$, in which $\mathbb{E} \subseteq \mathbb{N} \times \mathbb{N}$ is the edge set and $\mathbb{N} = \{1, 2, \dots, N\}$ presents the agents set. If there exists $(i, j) \in E$ and $(j, i) \in E$, \mathcal{G} is a connected undirected graph [18]. In this paper, each MG can exchange information with their neighbors by the connected undirected graph. Let \mathcal{A} be adjacency matrix and a_{ij} is element of the \mathcal{A} , if the MG i is directly connected with MG j , there is $a_{ij} = 1$, else, $a_{ij} = 0$. \mathcal{L} is defined as Laplacian matrix and $\mathcal{L} = \mathcal{D} - \mathcal{A}$ in which the degree matrix $\mathcal{D} = \text{diag} \left\{ \sum_{j=1}^N a_{1j}, \dots, \sum_{j=1}^N a_{Nj} \right\}$.

The projection operation is defined as [19]:

$$Pre_{\Pi_i}(p_i) = \begin{cases} p_i^{\min}, & p_i < p_i^{\min} \\ p_i, & p_i^{\min} \leq p_i \leq p_i^{\max} \\ p_i^{\max}, & p_i > p_i^{\max}. \end{cases} \tag{1}$$

where Pre_{Π_i} denotes the projection operator, $\Pi_i = \{p_i \mid p_i^{\min} \leq p_i \leq p_i^{\max}, \forall i \in \mathbb{N}\}$ and $\Pi = \prod_{i=1}^N \Pi_i$ denotes the cartesian product space.

Let ζ be a closed convex set, and point $\mathbf{x} \in \zeta$, then, the tangent cone to ζ is

$$\Gamma_{\zeta}(\mathbf{x}) \triangleq \left\{ \lim_{\epsilon \rightarrow \infty} \frac{\mathbf{x}_{\epsilon} - \mathbf{x}}{t_{\epsilon}} \mid \mathbf{x}_{\epsilon} \in \zeta, t_{\epsilon} > 0, \text{ and } \mathbf{x}_{\epsilon} \rightarrow \mathbf{x}, t_{\epsilon} \rightarrow 0 \right\} \tag{2}$$

The normal cone is

$$\Lambda_{\zeta}(\mathbf{x}) \triangleq \left\{ \vartheta \in R^N \mid \vartheta^T (\mathbf{y} - \mathbf{x}) \leq 0, \text{ for any } \mathbf{y} \in \zeta \right\} \tag{3}$$

Lemma 1 *There exists two closed convex sets $\xi_1, \xi_2 \subset R^N$, If $0 \in rint(\xi_1 - \xi_2)$, then, $\forall \mathbf{x} \in \xi_1 \cap \xi_2$, there is $\Gamma_{\xi_1 \cap \xi_2}(\mathbf{x}) = \Gamma_{\xi_1}(\mathbf{x}) \cap \Gamma_{\xi_2}(\mathbf{x})$ [17].*

There are a closed convex set Π and a convex map $f : \Pi \rightarrow R^N$. The VI (Π, f) denotes the variational inequality (VI), which is to seek the $\mathbf{x} \in R^N$ such that $(\mathbf{y} - \mathbf{x})^T f(\mathbf{x}) \geq 0, \forall \mathbf{y} \in \Pi$. The solution of VI is denoted by the set $SOL(\Pi, f)$, which can also be equivalently reformed by projection, namely $\mathbf{x} \in SOL(\Pi, f) \iff \mathbf{x} = Pre_{\Pi}(\mathbf{x} - f(\mathbf{x}))$.

Lemma 2 *Consider the VI (Π, f) based on the Lemma 1, the following two conclusions hold [20]:*

- (1) *Let Π be compact, then, $SOL(\Pi, f)$ is compact and nonempty;*
- (2) *Let Π be closed and $f(\mathbf{x})$ be strictly monotone, then, there is at most one solution for VI (Π, f) .*

3 Mathematic Modelling

Consider an energy scheduling MGS, which is constructed by the diesel generator unit, wind turbine unit and energy storage device. In this paper, we only consider one-hour energy scheduling and the mathematical cost models of all units are constructed as follows:

3.1 Diesel Generator Unit

Due to the intermittent power output of renewable clean energy, such as wind power generation, the diesel generator unit is an indispensable segment in the MG. Typically, the characteristics of the fuel consumption and power output are as follows [21]:

$$C_{dg} = c_{dg,1} (P_{dg})^2 + c_{dg,2} P_{dg} + c_{dg,3} \tag{4}$$

To improve the service life of the diesel generator, the output power P_{dg} should satisfy the following constraint:

$$P_{dg}^{\min} \leq P_{dg} \leq P_{dg}^{\max} \tag{5}$$

where P_{dg} denotes the output power of the diesel generator, $c_{dg,1}$, $c_{dg,2}$ and $c_{dg,3}$ are the cost parameters. P_{dg}^{\min} , P_{dg}^{\max} are respectively the minimum and maximum output power.

3.2 Wind Turbine Unit

Compared with diesel power generation, the advantage of wind power generation is the use of renewable clean energy. That can avoid the use of fossil fuels, reduce greenhouse gases, and greatly reduce the fuel cost in the process of power generation [22,23]. The wind power output is mainly dependent on the wind speed, and the available wind power generation P_{wt}^* can be quantized by the Weibull distribution curve [24].

$$P_{wt}^* = \begin{cases} 0, & v < v_{in} \text{ or } v > v_{out} \\ P^* \left(\frac{v-v_{ci}}{v^*-v_{ci}} \right)^3, & v_{in} < v < v^* \\ P^*, & v^* < v < v_{out} \end{cases} \tag{6}$$

where P^* is the rated power of the wind turbine unit. v , v_{in} , v^* , and v_{out} are the actual, cut-in, rated, and cut-out wind speed, respectively. Hence, the actual invoked wind power output P_{wt} should obey the following constraint.

$$0 \leq P_{wt} \leq P_{wt}^* \tag{7}$$

The maintenance cost of the wind turbine unit is as follows:

$$C_{wt} = c_{wt} \cdot P_{wt} \tag{8}$$

where c_{wt} denotes the unit maintenance cost.

3.3 Energy Storage Device

The energy storage device plays a key role in MG, which can curb the fluctuations in the renewable energy and loads. The cost function of the fuel cell can be denoted as:

$$C_{fc} = c_{fc} P_{fc} \tag{9}$$

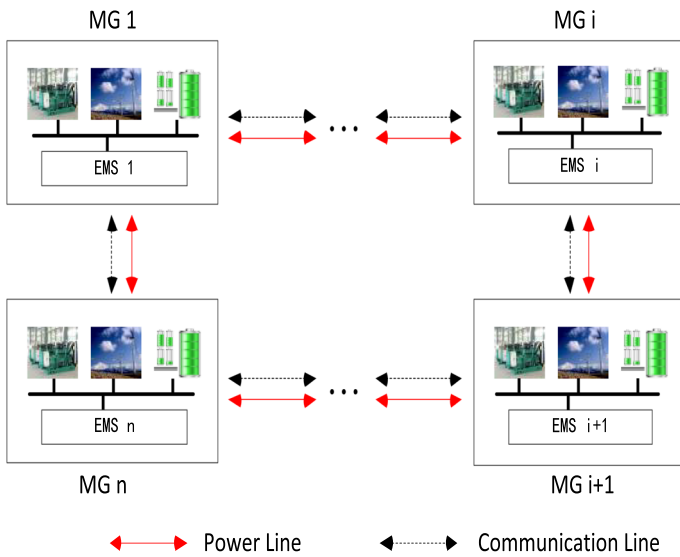


Fig. 1 The communication topology structure for the microgrid distribution network

where P_{fc} , c_{fc} are the power output and maintenance cost of the fuel cell, respectively.

To increase the using time of the battery, we should consider the state of charge (SOC) of the fuel cell [25]. Then, there is

$$SOC = SOC_0 + \eta \frac{P_{fc}}{B} \tag{10}$$

$$SOC^{\min} \leq SOC \leq SOC^{\max} \tag{11}$$

where SOC_0 , SOC^{\min} , SOC^{\max} , η , B denote separately the initial, minimum, maximum state of charge, charge/discharge conversion efficiency and the maximum battery capacity.

4 Energy Scheduling Game for the Microgrid Distribution Network

In this study, we consider a microgrid distribution network under the noncooperative game frame, the topological structure is shown in Fig. 1. Suppose that there is a set of the MG $\mathbb{N} = \{1, 2, \dots, N\}$, and the energy of the MG i is scheduled by the EMS i . The data information of each MG is known to neighbors completed by the undirected and connected graph. Hence, the privacy of the participants can be well protected.

4.1 Game Formulation

The profit function of MG i , $i \in \mathbb{N}$ is defined as

$$F_i(P_i, P_{-i}) = F_{s,i}(P_i, P_{-i}) - C_i(P_i) \tag{12}$$

(a) The operating income $F_{s,i}$

$$F_{s,i}(P_i, P_{-i}) = M^T P_i \left(c_{s,1} \sum_{i=1}^N M^T P_i + c_{s,2} \right) \tag{13}$$

where $M = 1_3$. The item $M^T P_i$ presents the total power output of the MG i , $c_{s,1} \sum_{i=1}^N M^T P_i + c_{s,2}$ denotes the power selling price, which is a function of the aggregate power output [15].

(b) The operating cost C_i

$$\begin{aligned} C_i &= C_{dg,i} + C_{fc,i} + C_{wt,i} \\ C_{dg,i} &= c_{dg,1} (P_{dg,i})^2 + c_{dg,2} P_{dg,i} + c_{dg,3} \\ C_{fc,i} &= c_{fc} P_{fc,i} \\ C_{wt,i} &= c_{wt} P_{wt,i} \end{aligned} \tag{14}$$

where $P_i = (P_{dg,i}, P_{fc,i}, P_{wt,i})^T \in R^3$.

Consider the equipment constraint of MG i , there is

$$P_{dg,i}^{\min} \leq P_{dg,i} \leq P_{dg,i}^{\max} \tag{15}$$

$$SOC_i = SOC_{0,i} + \eta_i \frac{P_{fc,i}}{B_i}$$

$$SOC_i^{\min} \leq SOC_i \leq SOC_i^{\max} \tag{16}$$

$$0 \leq P_{wt,i} \leq P_{wt,i}^* \tag{17}$$

Hence, the standard form of the noncooperative game for the proposed problem is as follows [26]:

$$\mathcal{G} = \{\mathbb{N}, \Pi, \{F_i\}_{i=1}^n\} \tag{18}$$

where $\mathbb{N} = \{1, 2, \dots, N\}$ is the MG set. Π_i is the strategy set of MG i , and there are $\Pi_i = \{P_i | (15) - (17)\}$ and $\Pi = \Pi_1 \times \dots \times \Pi_N$. F_i is the profit function of MG i .

Define the aggregate map of the proposed problem as [27]:

$$\Theta(P) = \frac{1}{N} \left(c_{s,1} \sum_{i=1}^N M^T P_i + c_{s,2} \right) \tag{19}$$

where $P = (P_1^T, \dots, P_N^T)^T \in R^{3N}$, $\Theta : R^{3N} \rightarrow R$.

Then, $\Theta(P)$ specifies the profit function $F_{s,i}(P_i, P_{-i})$ as $\Psi_i(P_i, \Theta(P)) : R^{3N+1} \rightarrow R$. $c_{s,1} \sum_{i=1}^N M^T P_i + c_{s,2}$ presents the local element to the aggregation. In addition, consider the balance of the power supply and demand, the constraint can be defined as:

$$\mathcal{K} = \left\{ P \in R^{3N} \mid \sum_{i \in \mathbb{N}} M^T P_i = \sum_{i \in \mathbb{N}} D_i \right\} = \left\{ P \in R^{3N} \mid \mathbb{M}^T P - D = 0 \right\} \tag{20}$$

where D presents the total power demand of all users, and there is $\mathbb{M} = (M^T, \dots, M^T)^T \in R^{3N}$. The feasible strategy set of game \mathcal{G} is $\Pi \cap \mathcal{K}$, \mathcal{K} is a set for the linear coupled constraints.

Definition 1 For such a game with coupled constraints, the point $P^* = (P_1^{*T}, \dots, P_N^{*T})^T$ is said to be GNE, if and only if, for all $i \in \mathbb{N}$, there is

$$F_i(P_i^*, P_{-i}^*) \geq F_i(x, P_{-i}^*), \quad \forall x \in \Pi_i \text{ and } (x, P_{-i}^*) \in \Pi \cap \mathcal{K} \tag{21}$$

Remark 1 As Eq. (13) states, the operating income of each MG is related to the power output. Under the noncooperative game frame, all MGs only care about their own profitability. They will comprehensively take their own operating cost and the other MGs' power output strategy into consideration, and schedule their own energy production to make the maximum profits.

4.2 Distributed Neurodynamic Algorithm for Seeking the GNE

In this part, we seek the GNE by a distributed neurodynamic algorithm, meanwhile, the correctness and convergence of the proposed algorithm will be analysed in the following.

Assumption 1 The Information exchanging between all MGs is allowed by a connected and undirected graph.

The distributed neurodynamic algorithm is designed to solve the problem, which is formulated as:

$$\begin{cases} \dot{P}_i = \text{Pre}_{\Pi_i} (P_i - \nabla_{P_i} F_i(P_i, P_{-i}) - \frac{\varrho}{N} M \lambda_i) - P_i \\ \dot{\lambda}_i = \gamma \sum_{j \in \mathbb{N}, j \neq i} \text{sgn}(\lambda_j - \lambda_i) + \mu (M^T P_i - D_i) \\ \dot{\kappa}_i = \alpha \sum_{j \in \mathbb{N}, j \neq i} \text{sgn}(\omega_j - \omega_i) \\ \dot{\omega}_i = \kappa_i + M^T P_i \end{cases} \tag{22}$$

where Pre_{Π_i} , ∇ and $\text{sgn}(\cdot)$ denote the projection operator, the gradient and the sign function, respectively. $\lambda_i(t) \in \mathbb{R}$, $\kappa_i(t) \in \mathbb{R}$. ϱ , γ and α are positive parameters, which satisfy $\alpha > (N - 1) \tilde{\psi}_1$ and $\gamma > \varrho(N - 1) \tilde{\psi}_2$.

The flow diagram of the proposed game algorithm is stated in Fig. 2. Each EMS of the MG will collect the required data, such as the power demand of all users and the actual wind speed. Consider the advantage of wind power generation is the use of renewable clean energy, the wind power output will be scheduled preferentially. Then, the power generation of the diesel generator and fuel cell as the backup power to compensate the wind power output. First, initialize the power output strategy $P(0)$, the iteration index $L = 1$, the small step size δ and the tolerant rate ε . The invoking of the neurodynamic algorithm can be stated as follows:

$$\begin{cases} P_i(t_{L+1}) = P_i(t_L) + \delta \dot{P}_i(t_L) \\ \lambda_i(t_{L+1}) = \lambda_i(t_L) + \delta \dot{\lambda}_i(t_L) \\ \kappa_i(t_{L+1}) = \kappa_i(t_L) + \delta \dot{\kappa}_i(t_L) \\ \omega_i(t_L) = \kappa_i(t_L) + M^T P_i(t_L) \end{cases} \tag{23}$$

The iteration will be end until $|P(t_{L+1}) - P(t_L)| < \varepsilon$ is satisfied, i.e. the strategy of each MG is unchanged or changed tinely.

For the $\tilde{\psi}_1$ and $\tilde{\psi}_2$, which are defined as [27]:

$$\begin{aligned} \tilde{\psi}_1 &\triangleq \sup_{y, z \in \Pi} \|y - z\| \\ \tilde{\psi}_2 &\triangleq \sup_{i \in \mathbb{N}} \left(\sup_{P_i \in \Pi_i} \|M^T P_i - D_i\| \right) \end{aligned} \tag{24}$$

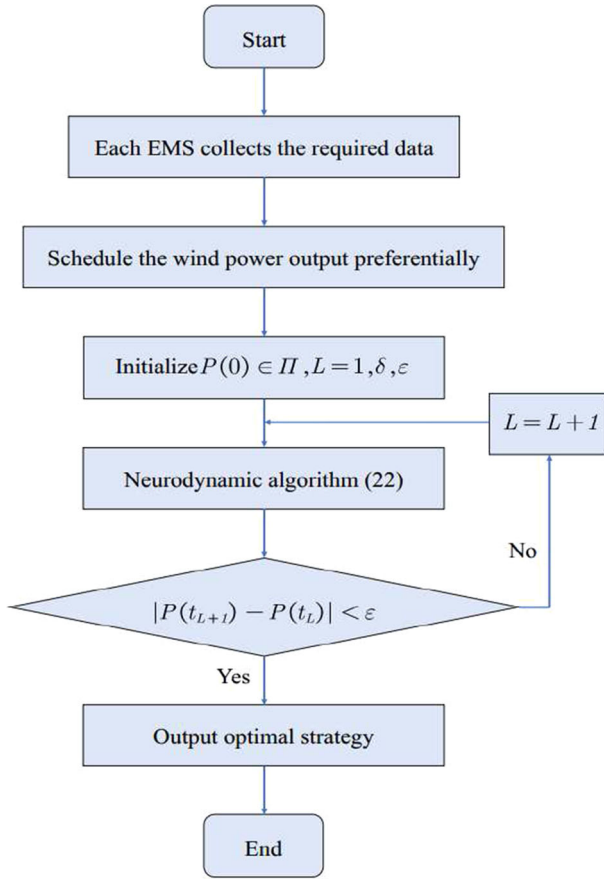


Fig. 2 The optimization process of the proposed game algorithm

The solution of the proposed algorithm (22) i.e., P^* , which can be well defined in the Filippov sense [28]. The initial conditions of (22) are given as follows:

$$P_i(0) \in \Pi_i, \lambda_i(0) = M^T P_i(0) - D_i, \kappa_i(0) = 0 \tag{25}$$

Lemma 3 *With the Assumption 1 and the conditions of $\alpha, \tilde{\psi}_1$ satisfied, then, $\lim_{t \rightarrow +\infty} \omega_i(t) - \frac{1}{N} \sum_{i=1}^N M^T P_i(t) = 0$ for $\forall i \in \mathbb{N}$ is exponential convergence for the following system [27].*

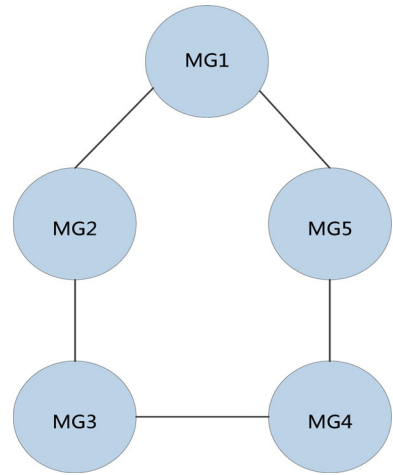
$$\begin{aligned} \dot{\kappa}_i(t) &= \alpha \sum_{j \in \mathbb{N}, j \neq i} \text{sgn}(\omega_j(t) - \omega_i(t)) \\ \omega_i(t) &= \kappa_i(t) + M^T P_i, \quad \kappa_i(0) = 0 \end{aligned} \tag{26}$$

Proof The proof is given in “Appendix A”. □

Lemma 4 *Consider the algorithm (22) under Assumption 1, and define*

$$\tilde{\lambda}(t) = \frac{\varrho}{N} \left(M^T P(0) - D + \int_0^t (M^T P(\tau) - D) d\tau \right) \tag{27}$$

Fig. 3 The information exchanging network for the microgrid distribution network



Therefore, for $\forall i \in \mathbb{N}$, $\|\omega_i(t) - \Theta(P(t))\| \rightarrow 0$, $\|\lambda_i(t) - \tilde{\lambda}(t)\| \rightarrow 0$ exponentially [27].

Suppose the set $\mathcal{E}^* \times \Psi^*$ is the solution of the following equation about $(P, \tilde{\lambda})$

$$\begin{aligned} 0 &= \text{Pre}_\Pi \left(P - \nabla_P F - \frac{\rho}{N} M \tilde{\lambda} \right) - P \\ 0 &= \frac{\rho}{N} (M^T P - D) \end{aligned} \tag{28}$$

and define the positive limit set of $(P(t), \tilde{\lambda}(t))$ is $\mathcal{E}^+ \times \Psi^+$.

Lemma 5 $\mathcal{E}^+ \times \Psi^+ \subseteq \mathcal{E}^* \times \Psi^*$ is satisfied, if and only if $\lim_{t \rightarrow 0} \dot{P}(t) = 0$ and $\lim_{t \rightarrow 0} \dot{\tilde{\lambda}}(t) = 0$ [29].

Proof The proof is given in ‘‘Appendix B’’. □

Theorem 1 If there exists $\tilde{\lambda}^* \in R^N$ and $(\tilde{\lambda}^*, P^*) \in \mathcal{E}^* \times \Psi^*$, then, P^* is the GNE of this paper.

Proof The proof is given in ‘‘Appendix C’’. □

Theorem 2 With the four conditions stated in Appendix C and Assumption 1 satisfied, the algorithm (22) is stable and converges to $\mathcal{E}^* \times \Psi^*$, then,

$$\begin{cases} \lim_{t \rightarrow \infty} \|\lambda_i(t) - \tilde{\lambda}(t)\| = 0, \forall i \in \mathbb{N} \\ \lim_{t \rightarrow \infty} \left\| \left(P(t), \tilde{\lambda}(t) \right) - \text{Pre}_{\mathcal{E}^* \times \Psi^*} \left(P(t), \tilde{\lambda}(t) \right) \right\| = 0 \end{cases} \tag{29}$$

Proof The proof is given in ‘‘Appendix D’’. □

Remark 2 Recently, the neurodynamic approach has been studied to solve the distributed optimization problem. Most existing distributed approaches only considered local constraints [7,30]. However, there is a need for real-time distributed algorithms with globally coupled

Table 1 The parameter values of the diesel generator unit in the simulation

MG i	$c_{s,1}$	$c_{s,2}$	Diesel generator unit					
			$P_{dg,i}^{\min}$ kw	$P_{dg,i}^{\max}$ kw	$c_{dg,1}$	$c_{dg,2}$	$c_{dg,3}$	
1	1.2	8.3	0	850	0.4	3	0	
2	1.2	8.3	0	800	0.4	3	0	
3	1.2	8.3	0	750	0.4	3	0	
4	1.2	8.3	0	650	0.4	3	0	
5	1.2	8.3	0	750	0.4	3	0	

Table 2 The parameter values of the energy storage device in the simulation

MG i	Energy storage device					
	$SOC_{0,i}$	SOC_i^{\min}	SOC_i^{\max}	c_{fc} RMB/kwh	η_i	B_i kwh
1	0.5	0.15	0.95	6	0.85	100
2	0.4	0.15	0.95	6	0.80	150
3	0.7	0.15	0.95	6	0.90	120
4	0.9	0.15	0.95	6	0.85	160
5	0.1	0.15	0.95	6	0.75	100

Table 3 The actual wind speed of the wind turbine unit in the simulation

MG i	00:00	00:15	00:30	00:45
1	4.863	4.638	4.324	5.062
2	5.39	5.186	4.943	5.778
3	5.39	5.186	4.943	5.778
4	4.724	4.391	4.515	4.828
5	4.848	5.057	4.905	4.772

constraints. Due to the parallel computation with theoretically certified optimality, neurodynamic distributed algorithms have the ability to deal with both local constraints and globally coupled constraints [8]. Hence, a distributed neurodynamic algorithm is designed to solve the proposed game problem with local constraints \mathcal{I} and a globally coupled constraint \mathcal{K} . Besides, compare with the heuristic algorithm, the advantage of the proposed algorithm is the theoretically certified optimality.

5 Simulation Example

In this section, we take 5 MGs into consideration to analyze the strategy selection of the energy scheduling game. Suppose that the given energy demands of all users are $D = 3500(\text{kwh})$. The information exchanging between all MGs is completed by a connected and undirected graph, see Fig. 3 and we can get the Laplacian matrix \mathcal{L} . Each MG presents an agent in the connected and undirected graph, the neighbor MGs can exchange information, but they can't get the information from the other MGs directly. The corresponding parameter values of the diesel generator and energy storage device are given in Tables 1 and 2 [31]. The rate

Table 4 The optimization values in the simulation

MG <i>i</i>	The optimization values				
	$P_{dg,i}^*$ kwh	$P_{fc,i}^*$ kwh	$P_{wt,i}^*$ kwh	SOC_i^*	$F_i^*(10^6)$ RMB
1	552.1	-29.8	129.8	0.2471	2.74
2	550.5	-30.0	235.4	0.2400	3.18
3	630.9	-59.4	235.4	0.2545	3.40
4	650.8	-88.4	113.1	0.3304	2.84
5	451.8	5.3	152.3	0.1513	2.56

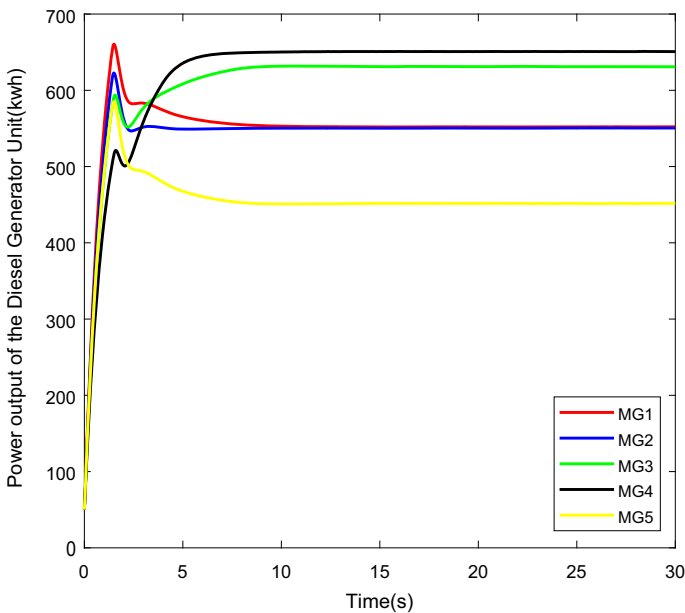


Fig. 4 The power output of the diesel generator unit of each MG under the specific strategy set

power, cut-in, rated, and cut-out wind speed are 100(KW), 2(m/s), 6(m/s) and 18(m/s), respectively [24]. The actual wind speed measurement is in a 15 min time interval, in this section, the cumulative wind power output in a 1 hour time interval is considered. An actual wind speed (Time: 00:00, 00:15, 00:30 and 00:45) obtained in Hubei province of China is shown in Table 3, and we set 10 (m), 30 (m), 30 (m), 50 (m), and 70 (m) anemometer towers as the wind turbine unit of the 5 MGs. The optimization values are given in Table 4.

$$\mathcal{L} = \begin{bmatrix} 2 & -1 & 0 & 0 & -1 \\ -1 & 2 & -1 & 0 & 0 \\ 0 & 2 & 2 & -1 & 0 \\ 0 & 0 & -1 & 2 & -1 \\ -1 & 0 & 0 & -1 & 2 \end{bmatrix}$$

Consider that the wind power output is scheduled preferentially, the power generation of the diesel generator and fuel cell as the backup power to compensate the wind power output.

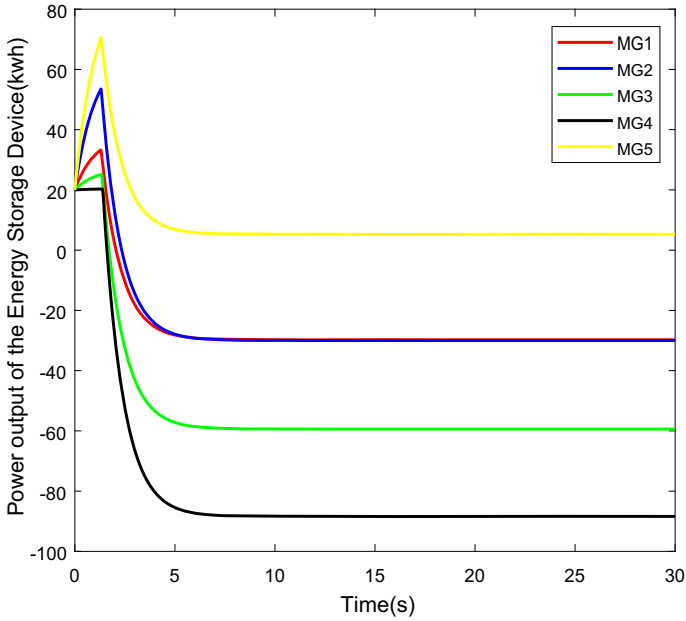


Fig. 5 The power output of the energy storage device under the specific strategy set

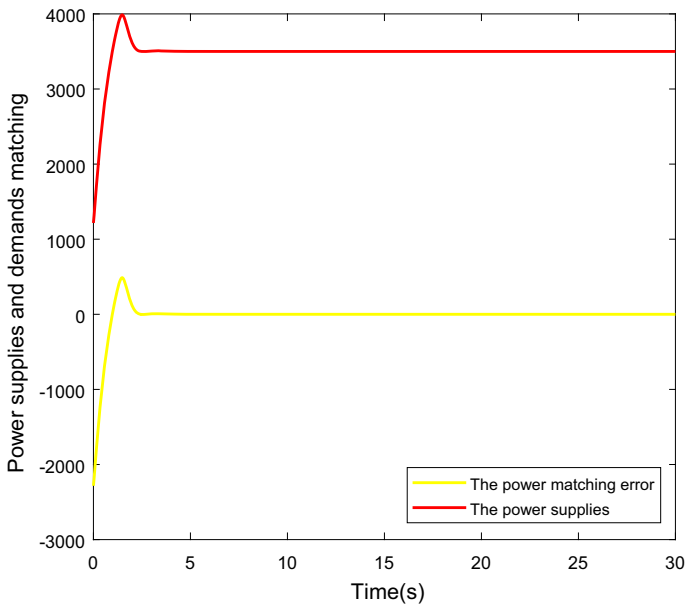


Fig. 6 The power supplies and demands matching during the optimization process

The cumulative wind power output of the 5 MGs are 129.8(kwh), 235.4(kwh), 235.4(kwh), 113.1(kwh) and 152.3(kwh), respectively. Figure 4 shows the optimization process of the

diesel generator unit output power through distributed optimization algorithm under the specific strategy set, and the detailed optimization values are given in Table 4.

Meanwhile, the corresponding constraints for the energy storage device are given in Table 2, i.e., the SOC of the fuel cell. The optimization process of the energy storage device output power is depicted in Fig. 5. For MG 5, the initial SOC is dissatisfied with the given constraint, which is recovered at the GNE. From the optimization values in Table 4, we can get that the different strategies (the constraints of the output power of diesel generator, initial, minimum, maximum state of charge of the fuel cell, etc. Each MG will choose different action to seek the maximum profit in the noncooperation game. With the exception of MG 5, the fuel cells of all other four MGs are discharging for maximum profit, the fuel cell of MG 5 is charging to satisfy the constraint. All participants will choose action in their own strategy set to seek the maximum profits.

Figure 6 gives the the power supplies and demands matching during the optimization process, the red line denotes the power supplies optimization process, which is fully equal to the given energy demand of the users. Moreover, the energy matching error tends to zero at the GNE, which explains the satisfaction of the equality constraint in this paper.

The simulation illustrates the effectiveness and feasibility of the proposed distributed optimization in addressing the proposed game problem.

6 Conclusion

In this paper, we considered a microgrid distribution network under the noncooperative game frame, which is an N -MGs competitive game. To maximize its profits, each MG should not only consider its strategy constraint but also the aggregate energy supplies of all MGs and the given energy demand of the users. Hence, the game with linear coupled constraints and distributed neurodynamic algorithm were proposed to seek the GNE. The correctness and convergence of the proposed algorithm were analyzed and the simulation example illustrated the effectiveness and feasibility of the proposed method.

Acknowledgements This work is supported by Natural Science Foundation of China (Grant Nos: 61773320), Fundamental Research Funds for the Central Universities (Grant No. XDJK2020TY003), and also supported by the Natural Science Foundation Project of Chongqing CSTC (Grant No. cstc2018jcyjAX0583).

Appendices

Appendix A: Proof of Lemma 3

Proof Since the Assumption 1 and the conditions of $\alpha, \tilde{\psi}_1$ are satisfied, and $\kappa_i(t)$ is strictly continuous, $\sum_{i=1}^N \dot{\kappa}_i(t) = 0$ is satisfied for all $t \geq 0$ such that $\sum_{i=1}^N \kappa_i(0) = 0$, then, there is $\sum_{i=1}^N \omega_i(t) = \sum_{i=1}^N M^T P_i(t)$. Furthermore, it is easy to obtain

$$\begin{aligned}
 (1) \quad & \sum_{i=1}^N \omega_i \sum_{j \in \mathbb{N}, j \neq i} \operatorname{sgn}(\omega_j - \omega_i) = \frac{1}{2} \sum_{(i,j) \in \mathbb{E}(t)} |\omega_i - \omega_j|; \\
 (2) \quad & |\kappa_q - \kappa_l| \leq \frac{1}{2} \sum_{(i,j) \in \mathbb{E}(t)} |\omega_i - \omega_j| \text{ for any } q \geq 1 \text{ and } l \leq N;
 \end{aligned}$$

$$\begin{aligned}
 (3) \quad \sum_{i=1}^N \left| \omega_i - \frac{1}{N} \mathbf{1}^T \omega \right| &\leq \frac{1}{N} \sum_{i=1}^N \sum_{j=1, j \neq i}^N |\omega_i - \omega_j| \\
 &\leq \frac{N-1}{2} \sum_{(i,j) \in \mathbb{E}(t)} |\omega_i - \omega_j|.
 \end{aligned}$$

Let $\varsigma(t) \triangleq \max \sum_{(i,j) \in \mathbb{E}(t)} |\omega_i - \omega_j|$ and $\omega(t) = \frac{1}{2} \|\omega(t) - \frac{1}{N} \mathbf{1}^T \omega(t)\|^2$. Then, for all $t \geq 0$, there is [32,33]

$$\begin{aligned}
 \omega(t) \neq 0, \dot{\omega}(t) &\leq -\frac{\alpha - (N-1) \tilde{\psi}_1}{2} \sum_{(i,j) \in \mathbb{E}(t)} |\omega_i - \omega_j| \\
 &\leq -\left(\alpha - (N-1) \tilde{\psi}_1\right) \varsigma(t) \leq 0
 \end{aligned} \tag{30}$$

where $\varsigma(t) \geq 0$ is completely continuous and $(\alpha - (N-1) \tilde{\psi}_1) \int_0^{+\infty} \varsigma(t) \leq \omega(0) < +\infty$, $\varsigma(t) \rightarrow 0$ as $t \rightarrow +\infty$. Then, for $t \geq \hat{t}$ and \hat{t} is sufficient large, there is $\omega(t) \leq \varsigma(t)$ and $\dot{\omega}(t) \leq (\alpha - (N-1) \tilde{\psi}_1) \omega(t)$, the prove is completed. \square

Appendix B: Proof of Lemma 5

If there is $\mathcal{E}^+ \times \Psi^+ \neq \emptyset$, then, for any $(P^+, \tilde{\lambda}^+) \in \mathcal{E}^+ \times \Psi^+$, $\{t_i\}_{i=1}^{+\infty}$ exists such that $\lim_{t \rightarrow +\infty} P(t_i) = P^+$ and $\lim_{t \rightarrow +\infty} \tilde{\lambda}(t_i) = \tilde{\lambda}^+$ [29,34]. Taking the the limit of t_i into Eqs. (22) and (27), we can get $(P^+, \tilde{\lambda}^+)$ is the solution of Eq. (28) according to the Lemma 2, and the prove is completed.

Appendix C: Proof of Theorem 1

Sufficiency. If $(\tilde{\lambda}^*, P^*) \in \mathcal{E}^* \times \Psi^*$, then, $P^* \in \Pi$ according to the definition of projection in the Sect. 2.2. We can also get $P^* \in \Pi^* \cap \mathcal{K}^*$ since $\mathbb{M}^T P^* - D = 0$. From Lemma 1, $P^* \in SOL(\Pi, \nabla_P F + \frac{\rho}{N} M \tilde{\lambda}^*)$, i.e., P^* is the GNE.

Necessity, If the P^* is the GNE, it seems easy to claim that there exist $\tilde{\lambda}^*$ and

$$-\nabla_P F(P^*) \in \frac{\rho}{N} M \tilde{\lambda}^* + \Lambda_\Pi(P^*) \tag{31}$$

with the following conditions satisfied [35,36]

- (1) $\forall i \in \mathbb{N}$, F_i is twice continuously differentiable;
- (2) $\nabla_P F$ is strictly monotone;
- (3) Π is compact and convex;
- (4) $0 \in \text{rint}(\Pi - \mathcal{K})$.

There exist a vector $\theta \in R^{2N}$ such that

$$\theta^T \nabla_P F(P^*) < 0 \tag{32a}$$

$$\mathbb{M}^T \theta = 0 \tag{32b}$$

$$\vartheta^T \theta \leq 0, \quad \forall \vartheta \in \Lambda_\Pi(P^*) \tag{32c}$$

then, from (32b) and (32c), $\theta \in \Gamma_{\Pi}(P^*) \cap \Gamma_{\mathcal{K}}(P^*) = \Gamma_{\Pi \cap \mathcal{K}}(P^*)$. According the definition of the tangent cone, there exist $P_{\epsilon} \in \Pi \cap \mathcal{K}$ and $t_{\epsilon} > 0$ such that $P_{\epsilon} \rightarrow P^*$, $t_{\epsilon} \rightarrow 0$, and $\lim_{\epsilon \rightarrow \infty} \frac{P_{\epsilon} - P^*}{t_{\epsilon}} = \theta$. Therefore

$$\theta^T \nabla_P F(P^*) = \lim_{\epsilon \rightarrow \infty} \frac{(P_{\epsilon} - P^*)^T \nabla_P F(P^*)}{t_{\epsilon}} \tag{33}$$

which conflicts with (32a), the prove is completed, the P^* is the unique GNE.

Appendix D: Proof of Theorem 2

For all $t > 0$, there is $\dot{P} \in \Gamma_{\Pi}(P)$, $P(t) \in \Pi$, and we also get

$$\dot{P}_i(t) = Pre_{\Pi_i} \left(P_i - \nabla_{P_i} F_i(P_i, P_{-i}) - \frac{\rho}{N} M \lambda_i \right) - P_i(t) + \phi_i(t) \tag{34}$$

where

$$\begin{aligned} \|\phi_i(t)\| &= \left\| Pre_{\Pi_i} \left(P_i - \nabla_{P_i} F_i(P_i, \Theta(P)) - \frac{\rho}{N} M \tilde{\lambda}_i \right) \right. \\ &\quad \left. - Pre_{\Pi_i} \left(P_i - \nabla_{P_i} F_i(P_i, P_{-i}) - \frac{\rho}{N} M \lambda_i \right) \right\| \\ &\leq \hat{\alpha} \left(\|\Theta(P) - \omega_i(t)\| + \|\tilde{\lambda}(t) - \lambda(t)\| \right) \end{aligned} \tag{35}$$

for some $\hat{\alpha} > 0$ and defining $\phi(t) = (\phi_1^T(t), \dots, \phi_N^T(t))^T$, then, $\phi(t)$ reduces exponentially based on the Lemma 2.

Let $\chi(t) = \begin{bmatrix} P(t) \\ \tilde{\lambda}(t) \end{bmatrix}$, $\nabla_P \tilde{F}(\chi) = \begin{bmatrix} \nabla_P F + \frac{\rho}{N} M \tilde{\lambda} \\ -\frac{\rho}{N} (M^T P - D) \end{bmatrix}$, $\mathcal{A} = \Pi \times R$, $\tilde{v}(\chi) = Pre_{\mathcal{A}} \left(\chi - \nabla_P \tilde{F}(\chi) \right)$ and $\chi^* \in \mathcal{E}^* \times \Psi^*$. Then, the Lyapunov function can be formulated as:

$$V(t) = (\chi - \tilde{v}(\chi))^T \nabla_P \tilde{F}(\chi) - \frac{1}{2} \|\chi - \tilde{v}(\chi)\|^2 + \frac{1}{2} \|\chi - \chi^*\|^2 \tag{36}$$

It is easy to get $V(t) \geq 0$. Moreover, the gradient of $V(t)$ is as follows

$$\dot{V}(t) = (\nabla_{\chi} V)^T \dot{\chi}(t) = (\nabla_{\chi} V)^T (\tilde{v}(\chi) - \chi) + \tilde{\phi}(t) \tag{37}$$

where $\tilde{\phi}(t) = [\phi(t), 0]^T \nabla_{\chi} V$. Π is bounded and according Lemma 4, $\phi(t)$ converges exponentially, then, $\|\tilde{\lambda}(t)\| \geq \tilde{\alpha}_1 + \tilde{\alpha}_2 t$ and $\|\tilde{\phi}(t)\| \leq (\tilde{\alpha}_3 + t \tilde{\alpha}_4) e^{-\tilde{\alpha}_5 t}$ for some constants $\tilde{\alpha}_1, \tilde{\alpha}_2, \tilde{\alpha}_3, \tilde{\alpha}_4, \tilde{\alpha}_5 > 0$. Hence,

$$\int_0^{+\infty} \|\tilde{\phi}(t)\| dt < +\infty \tag{38}$$

$$\dot{V}(t) \leq -(\chi - \chi^*)^T \left(\nabla_P \tilde{F}(\chi) - \nabla_P \tilde{F}(\chi^*) \right) + \tilde{\phi}(t) \tag{39}$$

As $t \rightarrow +\infty$, $\lim_{t \rightarrow +\infty} P(t) = P^*$ and $\limsup_{t \rightarrow +\infty} V(t) < +\infty$ such that $\tilde{\lambda}(t)$ is bounded, consequently, $\mathcal{E}^+ \times \Psi^+ \neq \emptyset$. From Eq. (27), there is $\lim_{t \rightarrow +\infty} \dot{\tilde{\lambda}}(t) = M^T P^* - D = 0$. Because of the trajectory of (22) is completely continuous and the right side of the (22) about $P(t)$ is consistently continuous in t . For $P(t)$ is convergent, $\lim_{t \rightarrow +\infty} \dot{P}(t) = 0$ according the Barbalat lemma, the prove is completed.

References

1. Wen S, Xiong W, Cao J et al (2020) MPC-based frequency control strategy with a dynamic energy interaction scheme for the grid-connected microgrid system. *J Franklin Inst* 357(5):2736–2751
2. Chen T, Jiang Y, Wang J et al (2020) Maintenance personnel detection and analysis using mask-RCNN optimization on power grid monitoring video. *Neural Process Lett* 51:1599–1610
3. Nazari-Heris M, Abapour S, Mohammadi-Ivatloo B (2017) Optimal economic dispatch of FC-CHP based heat and power micro-grids. *Appl Therm Eng* 114:756–769
4. Sardou IG, Zare M, Azad-Farsani E (2018) Robust energy management of a microgrid with photovoltaic inverters in VAR compensation mode. *Int J Electr Power Energy Syst* 98:118–132
5. Elsieid M, Oukaour A, Gualous H et al (2015) Energy management and optimization in microgrid system based on green energy. *Energy* 84:139–151
6. Liu Y, Li Y, Gooi HB et al (2019) Distributed robust energy management of a multi-microgrid system in the real-time energy market. *IEEE Trans Sustain Energy* 10(1):396–406
7. Liu Q, Le X, Li K (2019) A distributed optimization algorithm based on multiagent network for economic dispatch with region partitioning. *IEEE Trans Cybern.* <https://doi.org/10.1109/TCYB.2019.2948424>
8. Le X, Chen S, Li F et al (2019) Distributed neurodynamic optimization for energy internet management. *IEEE Trans Syst Man Cybern Syst* 49(8):1624–1633
9. Wang R, Li Q, Zhang B et al (2019) Distributed consensus based algorithm for economic dispatch in a microgrid. *IEEE Trans Smart Grid* 10(4):3630–3640
10. Li D, Deng L, Su Q et al (2020) Multimedia imaging model of information system based on self-organizing capsule neural network and game theory. *Neural Process Lett.* <https://doi.org/10.1007/s11063-020-10258-z>
11. Barrera J, Garcia A (2015) Dynamic incentives for congestion control. *IEEE Trans Autom Control* 60(2):299–310
12. Grammatico S (2017) Dynamic control of agents playing aggregative games with coupling constraints. *IEEE Trans Autom Control* 62(9):4537–4548
13. Wen S, Chen J, Wu Y (2020) CKFO: convolutional kernel first operated algorithm with applications in memristor-based convolutional neural networks. *IEEE Trans Comput Aided Des Integr Circuits Syst.* <https://doi.org/10.1109/TCAD.2020.3019993>
14. Li YZ, Zhao T, Wang P, Gooi H, Wu L, Liu Y, Ye J (2018) Cooperative operation of multi-microgrids via cooperative energy and reserve scheduling. *IEEE Trans Ind Inf* 14(8):3459–3468
15. Ye M, Hu G (2017) Game design and analysis for price-based demand response: an aggregate game approach. *IEEE Trans Cybern* 47(3):720–730
16. Liu Z, Wu Q, Huang S et al (2018) Optimal day-ahead charging scheduling of electric vehicles through an aggregative game model. *IEEE Trans Smart Grid* 9(5):5173–5184
17. Rockafellar RT, Wets RJB (1998) Variational analysis, volume 317 of Grundlehren der Mathematischen Wissenschaften. Fundamental Principles of Mathematical Sciences
18. West DB (2001) Introduction to graph theory. Prentice Hall, Upper Saddle River
19. Wen S, He X, Huang T (2020) Distributed neuro-dynamic algorithm for price-based game in energy consumption system. *Neural Process Lett* 51(1):559–575
20. Facchinei F, Pang JS (2003) Finite-dimensional variational inequalities and complementarity problems. Springer, Berlin
21. Li C, Yu X, Huang T et al (2018) Distributed optimal consensus over resource allocation network and its application to dynamical economic dispatch. *IEEE Trans Neural Netw Learn Syst* 29(6):2407–2418
22. Liu W, Gu W, Wang J et al (2018) Game theoretic non-cooperative distributed coordination control for multi-microgrids. *IEEE Trans Smart Grid* 9(6):6986–6997
23. Fu Y, Zhang Z, Li Z et al (2020) Energy management for hybrid AC/DC distribution system with microgrid clusters using non-cooperative game theory and robust optimization. *IEEE Trans Smart Grid* 11(2):1510–1525
24. Nojavan S, Zare K, Mohammadi-Ivatloo B (2017) Application of fuel cell and electrolyzer as hydrogen energy storage system in energy management of electricity energy retailer in the presence of the renewable energy sources and plug-in electric vehicles. *Energy Convers Manag* 136:404–417
25. Li C, Dong Z, Chen G et al (2018) Data-driven planning of electric vehicle charging infrastructure: a case study of Sydney. *IEEE Transactions on Smart Grid, Australia.* <https://doi.org/10.1109/TSG.2021.3054763>
26. Wen S, Xiong W, Tan J et al (2021) Blockchain enhanced price incentive demand response for building user energy network in sustainable society. *Sustain Cities Soc.* <https://doi.org/10.1016/j.scs.2021.102748>
27. Liang S, Yi P, Hong Y (2017) Distributed Nash equilibrium seeking for aggregative games with coupled constraints. *Automatica* 85:179–185

28. Di MM, Forti M, Nistri P et al (2016) Discontinuous neural networks for finite-time solution of time-dependent linear equations. *IEEE Trans Cybern* 46(11):2509–2520
29. Tian Y, Wang Z (2021) Composite slack-matrix-based integral inequality and its application to stability analysis of time-delay systems. *Appl Math Lett*. <https://doi.org/10.1016/j.aml.2021.107252>
30. Le X, Yan Z, Xi J (2017) A collective neurodynamic system for distributed optimization with applications in model predictive control. *IEEE Trans Emerg Top Comput Intell* 1(4):305–314
31. Li Z, Xu Y (2018) Optimal coordinated energy dispatch of a multi-energy microgrid in grid-connected and islanded modes. *Appl Energy* 210:974–986
32. Chen J, Wu Y, Yang Y et al (2020) An efficient memristor-based circuit implementation of squeeze-and-excitation fully convolutional neural networks. *IEEE Trans Neural Netw Learn Syst*. <https://doi.org/10.1109/TNNLS.2020.3044047>
33. Wen S, Ni X, Wang H (2021) Observer-based adaptive control for multiagent systems with unknown parameters under attacks. *IEEE Trans Neural Netw Learn Syst*. <https://doi.org/10.1109/TNNLS.2021.3051017>
34. Tan G, Wang Z, Li C (2020) *Hinf*ty performance state estimation of delayed static neural networks based on an improved proportional-integral estimator. *Appl Math Comput*. <https://doi.org/10.1016/j.amc.2019.124908>
35. Ding S, Xie X, Wang Z (2021) Periodic event-triggered synchronization for discrete-time complex dynamical networks. *IEEE Trans Neural Netw Learn Syst*. <https://doi.org/10.1109/TNNLS.2021.3053652>
36. Ding S, Wang Z, Rong N (2021) Intermittent control for quasi-synchronization of delayed discrete-time neural networks. *IEEE Trans Cybern* 51(2):862–873

Publisher's Note Springer Nature remains neutral with regard to jurisdictional claims in published maps and institutional affiliations.